# Environmental and geographical factors influence malaria transmission in KwaZulu-Natal province, South Africa

Osadolor Ebhuoma,[1,2] Michael Gebreslasie,[1] Oswaldo C. Villena,[3] Ali Arab[4]

[1]Department of Geography and Environmental Sciences, School of Agricultural, Earth, and Environmental Sciences, University of KwaZulu-Natal, Westville Campus, Durban, South Africa; [2]The Provincial Geospatial Centre, Environment and Protected Areas, Government of Alberta, Edmonton, Alberta, Canada; [3]The Earth Commons - Georgetown University's Institute for Environment & Sustainability, Georgetown University, Washington, DC, USA; [4]Department of Mathematics and Statistics, Georgetown University, Washington, DC, USA

Correspondence: Oswaldo C. Villena, The Earth Commons - Georgetown University's Institute for Environment & Sustainability, Georgetown University, 37th and O streets, Washington, DC 20057, USA.
E-mail: oswaldo.villena@georgetown.edu

Key words: malaria transmission, environmental variables, KwaZulu-Natal, zero-inflated models.

Conflict of interest: the authors declare that they have no competing interests.

Ethical approval: not required.

Availability of data and material: the datasets used and/or analyzed during the current study are available upon reasonable request from the corresponding author.

Funding: OE and MG were supported by the College of Agriculture, Engineering, and Science at the University of KwaZulu-Natal. AA and OCV were supported by the Earth Commons, Georgetown University's Institute for Environment & Sustainability. The funders had no role in the study design, data collection and analysis, decision to publish, or manuscript preparation.

Contribution: OE, MG, and AA, conceptualization; OE, MG, AA, and OCV, methodology, writing-review and editing; OE, AA, and OCV, formal analysis. All authors revised the manuscript and approved of its final version.

Acknowledgments: the authors would like to thank the College of Agriculture, Engineering and Science of the University of KwaZulu-Natal for the doctoral research bursary awarded to Osadolor Ebhuoma. We also thank the malaria control program of KwaZulu-Natal, South Africa for providing the data.

Received: 19 December 2024.
Accepted: 7 April 2025.


*Geospatial Health 2025; 20:1370*
*doi:10.4081/gh.2025.1370*



## Abstract

The malaria burden remains largely concentrated in sub-Saharan Africa. South Africa, a country within this region, has made significant progress toward malaria elimination. However, malaria continues to be endemic in three of its nine provinces: Limpopo, Mpumalanga, and KwaZulu-Natal (KZN), which are located in the northern part of the country and share borders with Botswana, Zimbabwe, and Mozambique. This study focuses on KZN, where district municipalities report monthly malaria cases ranging from zero to 8,981. Fitting Bayesian zero-inflated models in the INLA R package, we assessed the effects of various climate and environmental variables on malaria prevalence and spatio-temporal transmission dynamics from 2005-2014. Specifically, we analyzed precipitation, day and night land surface temperature, the Normalized Difference Vegetation Index (NDVI), the Enhanced Vegetation Index (EVI) and elevation data for KZN local municipalities. Our findings indicate that the best model was the Zero-Inflated Negative Binomial (ZINB) and that at 95% Bayesian Credible Interval (CI), NDVI (0.74; CI (0.95, 3.87) is significantly related to malaria transmission in KZN, with the north-eastern part of the province exhibiting the highest risk of malaria transmission. Additionally, our model captured the reduction of malaria from 2005 to 2010 and the following resurgence. The modelling approach employed in this study represents a valuable tool for understanding and monitoring the influence of climate and environmental variables on the spatial heterogeneity of malaria. Also, this study reveals the need to strengthen the already existing cross-border collaborations to fortify KZN's malaria elimination goals.

## Introduction

Malaria remains one of the most problematic vector-borne diseases in Africa despite long-term efforts fighting the disease. In 2023, the World Health Organization (WHO) reported 263 million malaria cases in the world, an increase of 11 million compared to 2022 and to 14 million in 2021 (WHO, 2024). Despite efforts eliminate this disease from its territory, South Africa has not been exempt from the rising case numbers, with most cases occurring along its northern borders with Mozambique, Zimbabwe and Botswana (Maharaj *et al*., 2019; Tsoka-Gwegni, 2022). One of these initiatives is the Southern Africa Development Community (SADC) Malaria Elimination Eight initiative (E8) established in 2009 with Angola, Botswana, Eswatini, Mozambique, Namibia, South Africa, Zambia and Zimbabwe with the goal to eliminate malaria from the 8 member countries by 2030 (Sikaala *et al.*,

2024). The northern regions of South Africa are the primary areas for malaria transmission in the country (Maharaj *et al*., 2019). This region includes the provinces of Limpopo, Mpumalanga, and KwaZulu-Natal (KZN), which share borders with Mozambique, the country that is the fourth major contributor of malaria cases on the African continent (WHO, 2023). The malaria parasite responsible for over 90% of malaria cases in the province is *Plasmodium falciparum*, with *Anopheles gambiae*, *An. arabiensis,* and *An. funestus* the major malaria vector species (Zianni *et al.*, 2013). Currently, KZN has only a 2% annual incidence of malaria cases, most of them in people from Mozambique who temporarily come to the informal border market (Raman *et al.*, 2020). This province experiences many imported cases driven by both formal and informal transport networks between South Africa and Mozambique. The continuous introduction of malaria into receptive areas by human population movement is a key factor in the failure of previous elimination campaigns (Tatem *et al.*, 2013). Besides human population movement at the border of KZN, it is important to consider the spatio-temporal delineation and prediction of malaria transmission, using relevant climate and environmental variables that could be key for malaria management programmes when shown as empirical maps of malaria risk and transmission.

Climate is a very important determinant of the spatio-temporal heterogeneity of malaria risk and transmission (Gao *et al.*, 2012; Garske *et al.*, 2013; Githeko, 2009; Midekisa *et al.*, 2015; Yé *et al.*, 2007; Zayeri *et al.*, 2011; Zinszer *et al.*, 2015). Temperature plays an integral role via complex interactions on malaria vector population dynamics and in parasite development within the vector (Craig *et al.*, 1999; Mordecai *et al.*, 2019; Villena *et al.*, 2022; Villena *et al.*, 2024b). Rainfall is another key component that contributes to malaria; its effect on malaria vector proliferation and malaria transmission intensity notably varies with rainfall amounts (Cairns *et al.*, 2012; White *et al.*, 2011; Zayeri *et al.*, 2011; Villena *et al*., 2024b).

While temperature and precipitation are widely acknowledged as major drivers of malaria prevalence, additional indicators, such as the Normalized Difference Vegetation Index (NDVI) and the Enhanced Vegetation Index (EVI) can also influence malaria dynamics by their quantification of vegetation greenness. For instance, studies have found that vegetation indices are positively correlated with mosquito abundance, mosquito community assembly and malaria prevalence (DanturJuri *et al*., 2015; Ferraguti, *et al.*, 2016; Ferraguti *et al.*, 2024). Other important geographic and environmental variables that have been widely reported in the literature for their influential role in malaria transmission are elevation, relative humidity, land use and land cover (Cohen *et al.*, 2008, 2010; Li *et al.*, 2013; Arab *et al*., 2014; Stefani *et al.*, 2013; Zayeri *et al.*, 2011). Furthermore, non-climatic factors, including human population movement, urbanization, socio-economy, demography and malaria interventions are also very important variables that impact malaria transmission dynamics (Ebhuoma *et al.*, 2017; Ernst *et al.*, 2009; Tatem *et al.*, 2013; Tatem *et al.*, 2008; Tusting *et al.*, 2013).

In this study, we explored the relationship of climate and environmental variables to malaria prevalence in KZN. Prevalence data had been collected in 14 local municipalities from 2005 to 2014. These data are the most extensive available on malaria prevalence in KZN but pose challenges for analysis due to the high number of non-malaria cases, since the data come from an area that it is in the process of malaria elimination. Reliable inferences and prediction of the spatio-temporal distribution of diseases depend on selecting an appropriate distribution for zero-inflated data. A flexible model that can handle the over-dispersion resulting from the excess zero values and still take account of the non-zero values is required (Neelon *et al.*, 2010). It is important that the zero values are considered in spatio-temporal modelling when dealing with a disease known for its spatio-temporal heterogeneity, including absence of cases increasingly observed in areas with progressing malaria elimination campaigns. This often presents valuable information related to the disease, such as the detection rate as well as the occurrence and knowledge of the disease by the population (Arab, 2015; Arab *et al.*, 2008). Varieties of zero-adjusted mixed models are available and they include the zero-inflated negative binomial (ZINB) model, Zero-Inflated Poisson (ZIP) model, Poisson hurdle model, and the negative binomial hurdle model (Arab, 2015; Arab *et al.*, 2008; Chipeta *et al.*, 2014; Neelon *et al.*, 2010; Villena *et al.*, 2024a). To address our research questions, we modelled and assessed the effects of precipitation, day and night Land Surface Temperature (LST), NDVI, EVI and elevation on malaria prevalence in the province of KZN. To fit our models, we used a set of various Bayesian spatio-temporal models that can handle zero-inflated malaria prevalence data such as the ZINB, ZIP, Poisson and negative binomial hurdle models (Kiani *et al.*, 2024; Villena *et al.*, 2024a). Our models accurately modelled zero-inflated malaria prevalence data against various environmental factors, providing a robust framework for understanding and forecasting malaria prevalence in KwaZulu-Natal, as well as across South Africa. This approach offers critical insights that can inform and enhance effective malaria management and prevention strategies, particularly in bordering regions with varying malaria prevalence gradients, toward the goal of malaria elimination.

## Materials and Methods

### Study area

The study took place in the three northern district municipalities (Umkhanyakude, Zululand and Uthungulu) in KZN. Umkhanyakude includes Jozini, uMhlabuyalingana, Big Five Hlabisa and Mtubatuba; Zululand eDumbe, uPhongolo, Abaqulusi, Ulundi and Nongoma; and Uthungulu Nkandla, Mthonjaneni, uMfolozi, uMhlathuze and uMlalazi (Figure 1). KZN is bordered by The Kingdom of Swaziland and The People's Republic of Mozambique in the North. It has a long shoreline along the Indian Ocean in the East and stretches down south-eastwards. The region possesses a sub-tropical climate with the majority of malaria incidence observed during October to May (the rainy months), with a seasonal peak usually in January and March (Moonasar *et al.*, 2012). The average annual rainfall ranges from 500 to 2,000 mm. Along the coastal areas, the summer temperatures are between 24°C to 32°C, and the mean winter temperature about 20°C. The Midlands generally possess a mild climate with relatively high summer rainfall and dry winters. The elevation of the region varies from sea level to over 3,000 m. The vegetation of the study area comprises coastal forest and thornveld along the coast. Towards the inlands, other forms of grassy vegetation takes over: lowveld, highland sourveld, Natal sour sandveld, valley bushveld and tall grassveld. Lowveld and thornveld characterise the low-lying hot and dry regions of northern KZN (Camp, 1999).

## Data

### *Malaria*

Malaria case data from January 2005 to December 2014 were obtained from the malaria control program of KZN. In South Africa, when a suspected malaria case presents, the blood smear of the suspected case is tested for *Plasmodium* using either microscopy or a rapid diagnostic test by a certified health officer (South Africa National Department of Health, 2012). If a positive result is obtained, patient details including patient demographics, the health facility where the case was reported, symptoms, malaria test results, diagnosis and treatment administered are entered into a malaria case notification form and reported to the relevant provincial malaria control programme. The details of malaria case are then fed into the malaria information system (South Africa National Department of Health, 2012). The distribution of malaria cases in KZN during the period of the study is characterised by an excess of areas with zero cases (about 81%) (Figure 2).

### *Environmental and geographical variables*

For each local municipality, we aggregated monthly and pentad, global, gridded precipitation, day and night LST, NDVI and EVI data from 2005 to 2014. Additionally, we included gridded elevation data in our models (Table 1). The raster datasets (*i.e.* Precipitation, NDVI, Elevation), which have different spatial resolutions, were imported into R version 4.2.2. and resampled if needed (Johnson *et al.*, 2021).

## Data analysis and models

A cross-correlation analysis was carried out to identify the suitable predictor variables to be put into the spatio-temporal models to guide against multicollinearity in the models and improve the model fit. We explored drivers of malaria transmission across a spatio-temporal gradient in KZN. Our malaria case data had excessive zeroes beyond what a common count distribution can fit, such as Poisson or negative binomial. For this study, we compared zero-inflated and hurdle models, which have been developed to handle zero-inflated data sets for count models like Poisson and the negative binomial. We fitted four models, the ZIP, the ZINB, the Poisson hurdle model and negative binomial hurdle model (Chipeta *et al.*, 2014; Arab, 2015; Villena *et al.*, 2024a).

### *The ZIP model*

This is a combination of a Poisson distribution part (non-zero component) and a point mass at zero (zero component). The zero data from an observation emerges from both the point mass at zero

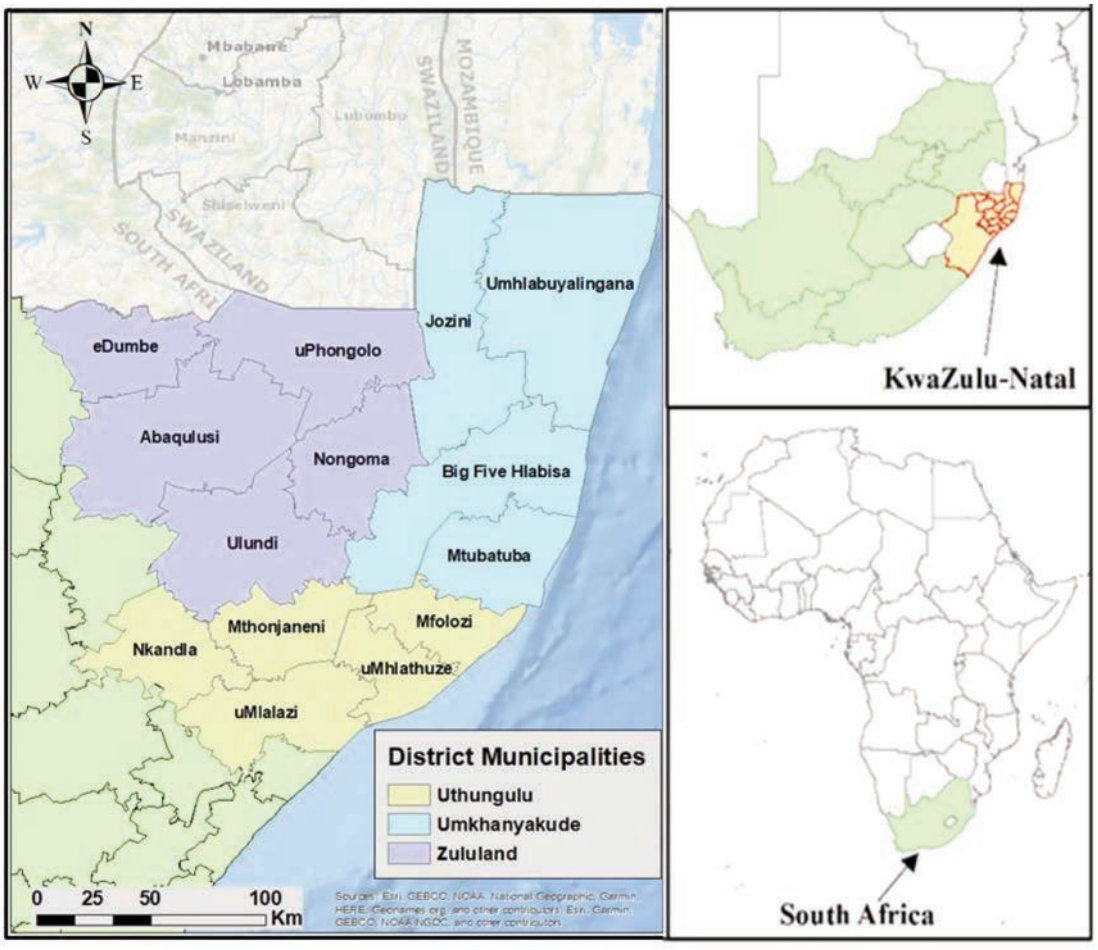


**Figure 1.** Map of the study area showing the malaria-endemic areas in KwaZulu-Natal, South Africa.

and the Poisson distribution. In the ZIP model, the zero component assumes a probability $p_i$ and the Poisson distribution assumes a probability 1 - $p_i$ where $i = 0, 1, 2, \ldots, n$. Thus, the ZIP model can be written as (see e.g., Chipeta *et al*., 2014):

$$(Y_i = 0) = p_i + (1 - p_i)\exp(-\lambda_i) \quad \text{Eq. 1}$$

$$(Y_i = k) = (1 - p_i)\frac{e^{-\lambda_i}\lambda_i^k}{k!},\ k = 1,2,\ldots \quad \text{Eq. 2}$$

where $p_i$ and $\lambda_i$ denote the probability of zero outcomes and the Poisson mean of non-zero outcomes, respectively; and $k$ denotes the value of possible none-zero outcomes. The effects of the predictors on the count distribution in a ZIP model can thus be evaluated by equations 3 and 4. The probability of excess zeros should be modelled employing a logistic regression as given in Eq. 3, while the impact of predictors on count data without the excess zeros can be modelled using Poisson regression presented in equation 4. The ZIP regression model links $p$ and $\lambda$ to the predictors, *i.e.*:

$$\text{logit}(p_i) = z_i\gamma \quad \text{Eq. 3}$$

$$\log(\lambda_i) = x_i\beta \quad \text{Eq. 4}$$

where log is the˙ natural logarithm function and the logit function defined as:

$$\text{logit}(p_i) = \log\left(\frac{p_i}{1 - p_i}\right).$$

## The ZINB model

This model can be described as a mixture of a mass of $p$ for the excess zeros and a mass of (1 -$p_i$) for the negative binomial distribution, where $0 \leq p_i \leq 1$. Thus, the ZINB model is written as (see *e.g.,* Chipeta *et al*., 2014):

$$P(Y_i = 0) = p_i + (1 - p_i)\left(\frac{\tau}{\tau+\lambda}\right)^{\tau},\ k = 0 \quad \text{Eq. 5}$$

$$P(Y_i = k) = (1 - p_i)\frac{\Gamma(\tau+k)}{k!\Gamma(\tau)}\left(\frac{\tau}{\tau+\lambda}\right)^{\tau}\left(\frac{\lambda}{\lambda+\tau}\right)^{k},\ k = 1,2,\ldots \quad \text{Eq. 6}$$

where $i = 1, 2, \ldots, n$, $x_i$ and $z_i$ are d- and q- dimensional vectors of predictors linked to the $i_{th}$ subject and $\beta$ and $\gamma$ the corresponding vectors of the regression parameters, respectively. Also, $p_i$ denotes the probability of zero outcomes, $\Gamma(.)$ is the Gamma function (*i.e.*, for integer $x$, $\Gamma(x) = (x - 1)!$ $\Gamma$ and $\lambda$ denote model parameters linked to mean and variance such that E(Y)= $\Gamma\lambda$ and Var(Y)= $\Gamma\lambda$ (1+).

## The Poisson Hurdle model

This model represents a two-part approach. The hurdle or logistic regression part models the zero *vs.* non-zero counts to obtain the zero probabilities. The second part is the zero truncated Poisson or regression part used to model the non-zero counts. Thus, the Poisson Hurdle model can be written as described by Chipeta *et al.*, (2014):

$$P(Y_i = 0) = p_i, \quad \text{Eq. 7}$$

$$P(Y_i = k) = (1 - p_i)\frac{\exp(-\lambda_i)\frac{(\lambda_i)^k}{k!}}{1 - \exp(-\lambda_i)},\ k = 1,2,\ldots \quad \text{Eq. 8}$$

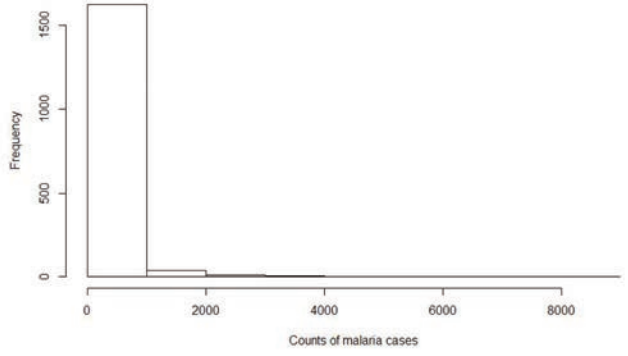


**Figure 2.** The counts of malaria cases in uMkhanyakude, uThungulu, and Zululand districts, South Africa (2005-2014).

**Table 1.** Environmental, and geographical variables.

| Variable | Description | Temporal resolution | Spatial resolution | Source |
|---|---|---|---|---|
| Precipitation | Pentad global gridded precipitation | Month | 2.5 X 2.5 degree | NOAA-NCEP |
| LSTD | Radiated daytime temperature at the Earth's surface | 8-day | 1 km | USGS-LP DAAC |
| LSTN | Radiated nighttime temperature at the Earth's surface | 8-day | 1 km | USGS-LP DAAC |
| NDVI | Measure of chlorophyll content as amount of vegetation 'greenness' | 16-day | 250 m | USGS-LP DAAC |
| EVI | Quantified vegetation 'greenness' corrected for atmospheric conditions and canopy background | 16-day | 250 m | USGS-LP DAAC |
| Elevation | Expressed as the Digital Elevation Model (DEM) | | 1 km | NOAA-GLOBE |

NDVI, the normalize difference vegetation index; EVI, the enhanced vegetation index; NOAA-NCEP, National Oceanic and Atmospheric Administration – National Centers for environmental Prediction; USGS-LP DAAC, U.S. Geological Survey – Land Processes Distributed Active Archive Center; NOAA-GLOBE, National Oceanic and Atmospheric Administration – Global Land One-km Base Elevation.

where symbols are those given above, with $p_i$ modelling all zeros. For this model, logistic regression should be employed in modelling the probability of zeros (Eq. 3), while the Poisson regression is the choice model to evaluate the impacts of predictors on positive count data (Eq. 4).

$$P(Y_i = 0) = p_i, \quad \text{Eq. 9}$$

$$P(Y_i = k) = (1 - p_i)\frac{\Gamma(k+\tau)}{\Gamma(k+1)\Gamma(\tau)} \times \frac{(1+\tau\lambda)^{-(k+\tau)}\tau^k\lambda^k}{1-(1+\tau\lambda)^{\tau}}, k = 1,2,3,\ldots \quad \text{Eq. 10}$$

The logistic regression should be employed in modelling the probability of zeros (Eq. 3), while the negative binomial regression is the choice model to evaluate the effects of predictors on count data (Eq. 4).

## Bayesian fitting of the spatio-temporal model

The Bayesian inference intuitively supports a hierarchical model approach, the implementation of which allows suitable data sampling variability, parameter uncertainty and likely spatial and temporal dependencies. Therefore, the effects of spatial and temporal dependencies are accounted for in the developed zero-inflated models. To this end, we formulated a hierarchical model for count data *Yi* 's (for $i$ =1, ..., $n$ ) and predictor variables *Xi*, ..., *Xp* following three modelling stages: i) data model, ii) process model and iii) parameter model (Arab, 2015).

i) The data model is written as:

$$Y_i \sim P(y_i|\theta_i, p), = i = 1, \ldots\ldots, n \quad \text{Eq. 11}$$

Let $P(y_i|_i, p)$ represent the probability mass function of a zero-inflated or hurdle distribution with model parameters $\theta_i$'s and mixture probability $p$.

ii) The process model is written as:

$$S(\theta_i) = \beta_0 + \beta_1 X_{1i} + \ldots + \beta_p X_{pi} + \gamma_i, \quad i = 1, \ldots\ldots, n \quad \text{Eq. 12}$$

where $S(.)$ represents a function specified based on the conditions on $\theta_i$'s; $\beta_i$ the spatial regression coefficients for the specified predictors *Xi*, ..., *X p*; $\gamma_i$ noise measurement; parameters $\gamma = (\gamma_1, \ldots., \gamma_n)$ the noise measurement based on the spatial dependence such that:

$$\gamma \sim N(0, \Sigma) \quad \text{Eq. 13}$$

$$\gamma \; N(0, \Sigma) \quad \text{Eq. 14}$$

where  represents the covariance matrix that explains the measure of the relationship each observation has with its neighbours (*i.e.* the spatial dependence of the data) and $\varphi$ a function of the strength of spatial relationship over spatial locations.  With  defined based on the geostatistical structure of the data and the spatial correlation specified based on an exponential covariogram model such that:

$$R(\varphi) = \exp(-\varphi d) \quad \text{Eq. 15}$$

where a symmetric spatial correlation is assumed based on the Euclidean distance between data points $d$ and a spatial range parameter, with $\varphi$ a function of the strength of spatial relationship over spatial locations.

iii) The parameter model:

The Bayesian approach regards parameter models as the prior distributions for the set of unknown parameters (e.g., $\beta_i$'s, $\tau$ and $\sigma^2$). This prior distribution and the traditional likelihood are combined to obtain the posterior distribution of the parameter of interest based on the statistical inference using Integrated Nested Laplace Approximation (INLA) via the Gaussian Markov Random Field (GMRF) (Blangiardo & Cameletti, 2015; Held *et al.*, 2010; Rue *et al.*, 2009). In this model, a flat non-informative prior distribution with a small mean and large variances were specified to all the unknown parameters. Refer to Ntzoufras (2008) and Gelman and Hill (2006) for more reviews on prior determination processes.

The cross-correlation matrix in Table 2 shows high correlation between $LST_N$ and Log-Precip, $LST_N$ and day $LST_D$, NDVI and EVI and night $LST_N$ and EVI. Thus, $LST_N$ and EVI were dropped so that a parsimonious model can be achieved, while Precipitation, $LST_D$, NDVI and Elevation were subsequently employed in the formulation of the spatio-temporal models. We fitted each spatio-temporal model using the R-INLA package (https://www.r-inla.org/; Rue *et al.*, 2099) in R (R Development Core Team, 2017). INLA is a method for approximate Bayesian inference that supports the evaluation of posterior margins in hierarchical models with latent random processes (Blangiardo & Cameletti, 2015; Held *et al.*, 2010; Gosoniu *et al.*, 2009; Rue *et al.*, 2009). The best model was selected based on the values *of the deviance information criterion* (DIC) and the Watanabe-Akaike Information Criterion (WAIC) as mentioned by Spiegelhalter *et al.* (2002). Using INLA and Stochastic Partial Differential Equations (SPDE), we built a mesh made up of triangles across the area of interest (study area) to evaluate the spatial fields (Figure 3).

**Table 2.** Correlation matrix of the predictor variables.

| | Log-Precip | Log-Elev | LSTD | LSTN | NDVIccc | EVI |
|---|---|---|---|---|---|---|
| Log-Precip | 1.00000 | -0.02719 | 0.48802 | 0.69111 | 0.50125 | 0.54121 |
| Log-Elev | | 1.00000 | -0.08536 | -0.31626 | -0.24264 | -0.28981 |
| $LST_D$ | | | 1.00000 | 0.64380 | -0.02312 | 0.07314 |
| $LST_N$ | | | | 1.00000 | 0.54455 | 0.60094 |
| NDVI | | | | | 1.00000 | 0.94630 |
| EVI | | | | | | 1.00000 |

Log-Precip, Log precipitation; Log-Elev, Log elevation; $LST_D$, daily land surface temperature; $LST_N$, land surface temperature at night; NDVI, Normalised difference vegetation index; EVI, Enhanced vegetation Index.

## Results

### Model comparisons

Based on DIC and WAIC values from the models (Table 3), the ZINB model (DIC = 5739.18; WAIC = 5762.25) was the best fit to our zero-inflated malaria prevalence dataset compared to the other three models. The second-best model was the negative binomial hurdle model (DIC = 6077.98; WAIC = 6083.60). The Poisson hurdle model had the weakest performance (DIC = 46053.40; WAIC = 66522.79). We, therefore, focused on the spatio-temporal ZINB model using NDVI as the only predictor variable in subsequent parts of the results and discussion sections (Table 4).

### Posterior inference

The ZINB analysis results in Table 3 indicates that at 95% CI, NDVI is significant and lies within positive values. This implies that the regression parameter NDVI significantly increases the zero-inflation probability *i.e.* they are more likely to correspond to excess zeros. In other words, higher probability of observing a zero count of malaria is associated with lower NDVI (0.74; 95% CI (0.95, 3.87), while Precipitation, $LST_D$ and Elevation were not statistically significant.

The map of posterior means (Figure 4A) indicated a high risk of malaria morbidity in the northern central and north-eastern parts of the study area including the local municipalities of Jozini, Umhilabuyalingana, Big Five Hlabisa in the district of Umkhanyakude; uPhongolo, Nongoma, Ulundi in the district of Zululand; and uMlalazi in the district of Uthungulu. The areas with lowest malaria risk were the local municipalities of Mtubatuba and Mfolozi. The map of posterior standard deviations (Figure 4B) indicates the varying level of uncertainty across the province. The highest posterior errors across the province are at the periphery or borders of the local municipalities.

The temporal random effects (Figure 5) present the estimated trend of malaria prevalence with associated 95% prediction intervals for the district municipalities of uMkhanyakude, uThungulu and Zululand. We observed a constant decline of malaria prevalence from 2005 to 2010, after which there was a resurgence of malaria prevalence. The 95% CI for prediction provided information about the uncertainty around the low and declining estimates of malaria prevalence in the study area.

### Summary outcome

This study provided evidence that there is still high risk of malaria transmission in its northern district municipalities of KZN that share borders with the African countries of Mozambique and Eswatini. More specifically in the local municipalities of Jozini, Umhilabuyalingana, Big Five Hlabisa in the district of Umkhanyakude; uPhongolo, Nongoma, and Ulundi in the district of Zululand; and in uMlalazi in the district of Uthungulu. Malaria surveillance and response must remain a priority, as the achievement of malaria elimination in KZN is under threat from multiple factors such as malaria importation from neighbouring countries that share borders with KZN (Raman *et al.*, 2020), climate change (Caminade *et al.*, 2014), insecticide resistance (Zinszer and Talisuna, 2022), and the expansion in range of the *Anopheles*

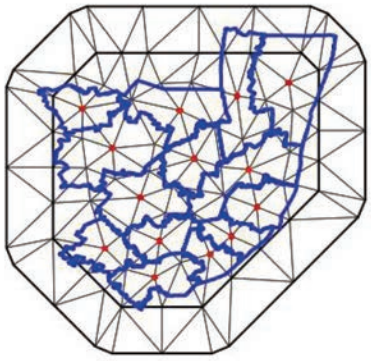

**Figure 3.** INLA/SPDE mesh for the spatial fields.

**Table 3.** Comparison of zero-inflated spatio-temporal models based on their DIC and WAIC values.

| Spatio-temporal Model | DIC | WAIC |
|---|---|---|
| ZINB | 5739.18 | 5762.25 |
| ZIP | 45910.78 | 66275.76 |
| Negative Binomial Hurdle | 6077.98 | 6083.60 |
| Poisson Hurdle | 46053.40 | 66522.79 |

DIC, the Deviance Information Criterion; WAIC, the Watanabe-Akaike information Criterion; ZINB, Zero inflated negative binomial; ZIP, Zero inflated Poisson.

**Table 4.** Posterior summary statistics for the zero-inflated negative binomial model for malaria prevalence in KwaZulu-Natal.

| Coefficient estimate | Standard error | 2.5th percentile | Mean | 97.5th percentile |
|---|---|---|---|---|
| Intercept | 8.9484 | -18.5891 | -0.5214 | 17.4483 |
| Log-Precip | 0.0763 | -0.0741 | 0.0762 | 0.2256 |
| NDVI | 0.7411 | 0.9513 | 2.4141 | 3.8656 |
| $LST_D$ | 0.0212 | -0.0238 | 0.0176 | 0.0595 |
| Log-Elev | 1.5194 | -3.2153 | -0.1504 | 2.9024 |

Log-Precip, Log precipitation; NDVI, Normalised difference vegetation index; $LST_D$, daily land surface temperature; Log-Elev, Log elevation.

*stephensi* invasive mosquito in Africa (Sinka *et al.*, 2020, Villena *et al.*, 2022). The ZINB model was identified as the best model for the over-dispersed, excess zeros and the spatio-temporal dependencies of the malaria case data in the malarious areas of KZN after considering the influence of climate variables. The results of the posterior statistics from the ZINB model indicate a significant relationship between NDVI and malaria cases. In addition, the malaria spatio-temporal risk map suggests a functional malaria control system that maintains relatively low malaria morbidity across KZN; however, the north-eastern part of the province still has a high risk of malaria transmission. These results are consistent with malaria risk maps developed by the South Africa department of health in 2007 and 2013 using the geographical distribution of confirmed malaria cases (Morris *et al.*, 2013). Thus, improved health management strategies and targeted additional interventions are required to achieve significant malaria risk reduction amongst the most vulnerable areas and populations.

## Discussion

To adequately address the issue of over-dispersion arising from the excess zero or zero-inflated spatio-temporal malaria data there is need for using appropriate models such as zero-inflated models and/or hurdle models. In the literature some authors find that ZINB models are the best to deal with zero-inflation data while others find that the ZIP or hurdle models are the best. For example, the study of Villena *et al.* (2024a) found that the ZINB was the best model to assess zero-inflated abundance of *Culex quinquefasciatus* mosquitoes which transmit avian malaria in honeycreepers in Hawaii. Also, a Bayesian geostatistical Zero-Inflated Binomial (ZIB) climatic model formulated by Giardina *et al.* (2012) suggested a significant relationship between NDVI and night with malaria in Senegal, while a study by Kasasa *et al.* (2013), showed how two different zero-adjusted models were needed to understand the malaria transmission patterns in a small area in Northern Ghana. The Bayesian geostatistical ZIB and ZINB approaches were used to evaluate the sporozoite rate and mosquito densities, respectively

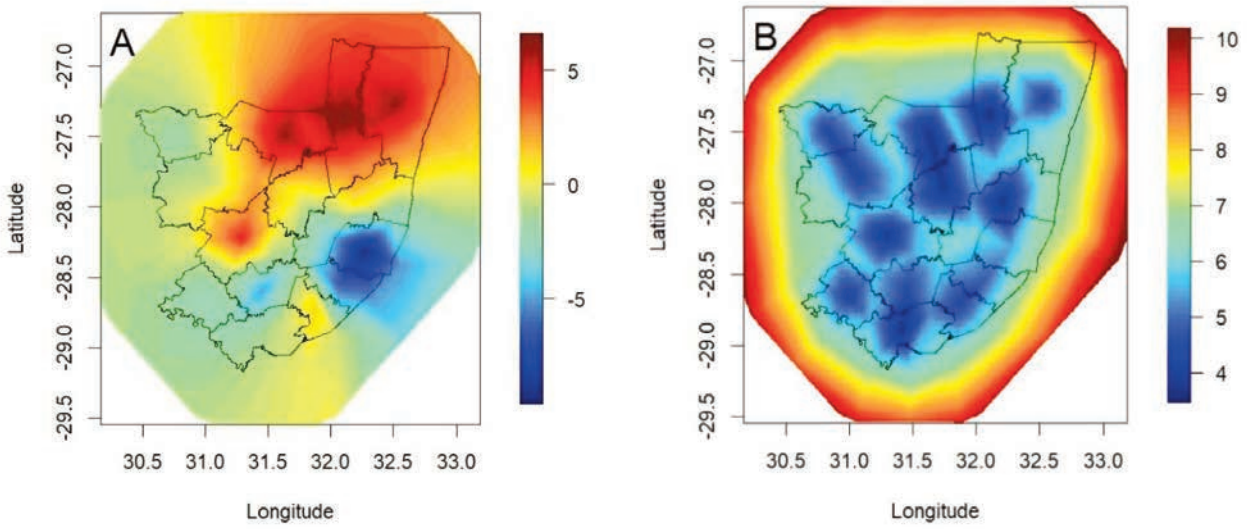


**Figure 4.** Posterior mean (**A**) and posterior standard deviation (**B**) of malaria prevalence in KwalaZulu-Natal, South Africa during 2005-2014.

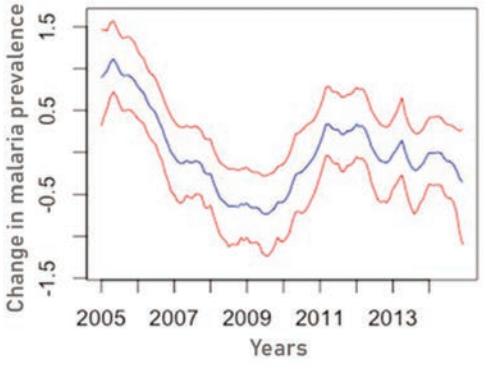


**Figure 5.** Posterior mean (blue line) and 95% credible intervals (red lines) of malaria prevalence in KwalaZulu-Natal, South Africa during 2005-2014.

revealing that a significant spatio-temporal heterogeneity of entomological inoculation rate estimates and malaria transmission intensity existed in the small area (Kasasa *et al.*, 2013).

The ZIP model, on the other hand, was a suitable model for mapping malaria incidence data with excess zeros in Afghanistan (Alegana *et al.*, 2014) and Northern Namibia (Alegana *et al.*, 2013). Similarly, the ZIP model was considered the desirable model for developing a spatio-temporal HIV/TB model in South Africa's Northeast (Musenge *et al.*, 2013), and an HIV model in New York, USA (Musal and Aktekin, 2013) using mortality data with excess zeros. Alegana *et al.* (2013) also employed a Bayesian ZIP approach to model the malaria incidence risk in northern Namibia, considering tropical rainfall measuring data on rainfall, temperature suitability and EVI data. The multivariate analysis revealed that only EVI was significant and the predicted malaria risk map suggested that areas bordering Angola and Zambia were at the highest risk of malaria transmission. A similar study was conducted in Afghanistan, in which the same Bayesian approach with climate and environmental variables was used to model the incidence of *Plasmodium vivax* and *P. falciparum* at the district level (Alegana *et al.*, 2014). The multivariate analysis based on the *P. vivax* model revealed that only the temperature suitability index was significant, but none of the climatic and environmental variables were significant based on the *P. falciparum* model. The predicted malaria risk map suggested that the eastern and south-eastern Afghanistan areas bordering Pakistan were at the highest risk of malaria incidence. Other studies compared different zero-inflated models and the best-fit model was identified by relevant comparative measure(s). For instance, Neelon *et al.* (2010) compared the Poisson, Poisson hurdle, ZIP and Zero-altered Poisson models. Based on the DIC value and the negative cross-validatory log likelihood measures, the ZIP model produced the best fit model. Also, Arab (2015) compared the Poisson Hurdle model, ZIP, Poisson Hurdle with the probability, Negative binomial Hurdle, ZINB and Negative Binomial Hurdle models. In this case, ZIP was reported to have the lowest DIC value.

The ZINB model formulated in this study, suggests that the relevance of NDVI in malaria transmission modelling cannot be overemphasised. NDVI can be used to assess the level of greenness of a vegetation (Hay *et al.*, 1998; Midekisa *et al.*, 2012), but not only that, it can also serve as a proxy for precipitation, near-surface humidity, and surface water (Hay *et al.*, 1998; Midekisa *et al.*, 2012). NDVI has been identified as the most important predictor in malaria transmission modelling across sub-Saharan Africa (Ebhuoma & Gebreslasie, 2016). Some studies conducted across these countries have shown that increase in vegetation indices can be used to predict increase in malaria risk (Gosoniu *et al.*, 2010; Nygren *et al.*, 2014; Sogoba *et al.*, 2007). Contrarily, a previous study conducted in Senegal (Giardina *et al.*, 2012) showed that an increase in NDVI was associated with low malaria risk. The relationship between NDVI and malaria in this study can be explained by the fact that NDVI has constantly been reported to be associated with precipitation, near-surface humidity and surface water (Hay *et al.*, 1998; Midekisa *et al.*, 2012). However, the strength or form of the relationship is dependent on the structure of the ecosystem. For this reason, the effect of rainfall in high amounts have on vector can also be related to high NDVI values. Although NDVI can provide information on vegetation intensity, it loses sensitivity over denser vegetation. In light of this characteristic, EVI is suggested to be a reliable substitute (Huete *et al.*, 2002; Matsushita *et al.*, 2007; Viña *et al.*, 2004). However, in this study, EVI was dropped in the preliminary phase of the analysis to guide against multicollinearity.

The uncertainties attributed to relying solely on climatic and environmental determinants to predict malaria disease make it challenging for malaria surveillance and intervention efforts (Adu-Prah & Tetteh, 2015). For this reason, in addition to the climatic and environmental inference provided by the spatio-temporal Bayesian ZIP modelling in this study, a map which can further guide the malarial interventional programmes in KZN was produced. This malaria risk map showed that there was a hotspot in the north-eastern region of KZN bordering Swaziland and Mozambique between the years 2005–2014, which supports similar patterns obtained from previously developed malaria risk maps (Morris, *et al.*, 2013). Jozini and uMhlabuyalingana local municipalities were identified as the areas with the highest malaria transmission risk. The elevated risk can, to some extent, be attributed to population movement between neighbouring countries, a fact that poses a significant challenge to achieving zero local transmission. Such movement patterns typically originate from regions with high transmission and spread to regions with low transmission. Our study has also certain limitations, including the lower sensitivity of microscopy and rapid detection tests compared to more advanced methods such as quantitative real-time Polymerase Chain Reaction test (qPCR), variations in intervention coverage, unreported asymptomatic cases, and confounding factors such as socio-demographic variables.

This study provides evidence to support the renewed cross-border collaborative efforts with the MOSASWA (Mozambique, South Africa and Swaziland) malaria initiative instituted in 2015 (Moonasar *et al.*, 2016). The initiative aims to boost the progress made by the participating nations towards achieving zero local transmission by further strengthening collaboration between relevant academic institutions, sharing expertise, channelling intervention resources to vulnerable populations in the region (especially the mobile population and border populations) and sourcing for long-term financial support (Moonasar *et al.*, 2016). Additionally, participating nations should enhance cooperation in surveillance, multi-country intervention programs, and data sharing to monitor progress toward malaria elimination and adjust future strategies accordingly. In addition to the MOSASWA initiative proposed to facilitate KZN's and South Africa's malaria programme transition from pre-elimination to elimination, a modelling approach which takes account of the effects of population movement between the MOSASWA countries and from other malaria endemic countries is important. This will help understand the spatial and temporal implications of mobile population in high transmission areas. It will also serve as a guide for adequate dissemination of chemoprophylaxis message to mobile populations and travellers in malarious and non-malarious areas, and for setting up a quick response strategy with regard to imported cases. Ultimately, it will result in timely channelling of malaria intervention resources to handle the threats that may arise from potential imported cases. Also, the KZN malaria programme should be further strengthened and expanded by conducting routine genotyping of vectors, improved insecticide resistance monitoring, close monitoring of intervention resources to ensure adequate implementation, and formation of malaria elimination commissions to provide technical and managerial guidance to malaria programmes at all levels (district, provincial and national).

## Conclusions

The aim of the malaria programme in KZN is to develop elimination strategies followed by eradication strategies. The low and excess zero prevalence recorded in the malarious local municipalities revealed that the Bayesian spatio-temporal zero-inflated models can serve as a suitable tool for the relevant policy makers. Thus, spatio-temporal ZINB Bayesian modelling and the map produced in this study present valuable tools for understanding and monitoring the influence of climate variability on the spatial heterogeneity of malaria in KZN. They can play a significant role in the management, prioritizing and allocation of intervention resources according to transmission variabilities. Also, this study has revealed the importance of strengthening the already existing cross-border collaborations for the fortification of KZN's malaria elimination target.

## References


Adu-Prah S, Tetteh EK, 2015. Spatiotemporal analysis of climate variability impacts on malaria prevalence in Ghana. Appl Geogr 60:266-273.

Alegana V, Wright J, Nahzat S, Butt W, Sediqi AW, Habib N, 2014. Modelling the incidence of Plasmodium vivax and Plasmodium falciparum malaria in Afghanistan 2006–2009. PLoS ONE 9:e102304

Alegana VA, Atkinson PM, Wright JA, Kamwi R, Uusiku P, Katokele S, SnowRW, Noor A M, 2013. Estimation of malaria incidence in northern Namibia in 2009 using Bayesian conditional-autoregressive spatial-temporal models. Spat Spatiotemporal Epidemiol 7:25-36.

Arab A, 2015. Spatial and spatio-temporal models for modeling epidemiological data with excess zeros. Int J Environ Res Public Health 12:10536-48.

Arab A, Jackson MC, Kongoli C, 2014. Modelling the effects of weather and climate on malaria distributions in West Africa. Malar J 13:126.

Arab A, Wildhaber ML, Wikle CK, Gentry CN, 2008. Zero-inflated modeling of fish catch per unit area resulting from multiple gears: application to channel catfish and shovelnose sturgeon in the Missouri River. N Am J Fish Manag 28:1044-1058.

Blangiardo M, Cameletti M, 2015. Spatial and spatio-temporal Bayesian models with R-INLA, John Wiley & Sons, 308 pp.

Cairns M, Roca-Feltrer A, Garske T, Wilson AL, Diallo D, Milligan PJ, Ghani AC, Greenwood BM, 2012. Estimating the potential public health impact of seasonal malaria chemoprevention in African children. Nat Commun 3:881.

Caminade C, Kovats S, Rocklov J, lloyd S, 2014. Impact of climate change on global malaria distribution. PNAS 111:3286-3291.

Camp KGT, 1999. A Bio-Resource Classification for KwaZulu-Natal, South Africa. University of Natal, Pietermaritzburg, South Africa, 140 pp.

Chipeta MG, Ngwira BM, Simoonga C, Kazembe LN, 2014. Zero adjusted models with applications to analysing helminths count data. BMC Res Notes 7:856.

Cohen JM, Ernst KC, Lindblade KA, Vulule JM, John CC, Wilson M L, 2010. Local topographic wetness indices predict household malaria risk better than land-use and land-cover in the western Kenya highlands. Malar J 9:328.

Cohen JM, Ernst KC, Lindblade KA, Vulule JM, John CC, Wilson ML, 2008. Topography-derived wetness indices are associated with household-level malaria risk in two communities in the western Kenyan highlands. Malar J 7:40.

Craig MH, Snow R, le Sueur D, 1999. A climate-based distribution model of malaria transmission in sub-Saharan Africa. Parasitol Today 15:105-111.

Dantur Juri MJ, Estallo E, Almirón W, Santana M, Sartor P, Lamfri M, Zaidenberg M, 2015. Satellite-derived NDVI, LST, and climatic factors driving the distribution and abundance of Anopheles mosquitoes in a former malarious area in northwest Argentina. J Vector Ecol 40:36-45.

Ebhuoma O, Gebreslasie M, 2016. Remote sensing-driven climatic/environmental variables for modelling malaria transmission in Sub-Saharan Africa. Int J Environ Res Public Health 13:584.

Ebhuoma O, Gebreslasie M, Magubane L, 2017. Modeling malaria control intervention effect in KwaZulu-Natal, South Africa using intervention time series analysis. J Infec Public Health 10:334-8.

Ernst KC, Lindblade KA, Koech D, Sumba PO, Kuwuor DO, John CC, Wilson ML, 2009. Environmental, socio-demographic and behavioural determinants of malaria risk in the western Kenyan highlands: a case-control study. Trop Med Int Health 14:1258-65.

Ferraguti M, Magallanes S, Mora-Rubio C, Bravo-Barriga D, de Lope F, Marzal A, 2024. Landscape and climatic factors shaping mosquito abundance and species composition in southern Spain: A machine learning approach to the study of vector ecology. Ecol Infor 84: 102860.

Ferraguti M, Martinez-de la Puente J, Roiz D, Ruiz S, Soriguer R, Figuerola J, 2016. Effects of landscape anthropization on mosquito community composition and abundance. Sci Rep 6: 29002.

Gao HW, Wang LP, Liang S, Liu YX, Tong SL, Wang JJ, Li YP, Wang XF, Yang H, Ma JQ, Fang LQ, Cao WC, 2012. Change in Rainfall Drives Malaria Re-Emergence in Anhui Province, China. PLoS ONE 7:e43686.

Garske T, Ferguson NM, Ghani AC, 2013. Estimating air temperature and its influence on malaria transmission across Africa. PLoS ONE 8:e56487.

Gelman A, Hill J, 2006. Data analysis using regression and multilevel/hierarchical models, Cambridge University Press, 648 pp.

Giardina F, Gosoniu L, Konate L, Diouf MB, Perry R, Gaye O, Faye O, Vounatsou P, 2012. Estimating the burden of malaria in Senegal: Bayesian zero-inflated binomial geostatistical modeling of the MIS 2008 data. PLoS ONE 7:e32625.

Githeko AK, 2009. Malaria And Climate Change. Commonwealth Health Minister's, Commonwealth Secretariat, 42-45 pp.

Gosoniu L, Veta AM,Vounatsou P, 2010. Bayesian geostatistical modeling of Malaria Indicator Survey data in Angola. PLoS ONE 5:e9322.

Gosoniu L, Vounatsou P, Sogoba N, Maire N, Smith T, 2009. Mapping malaria risk in West Africa using a Bayesian nonparametric non-stationary model. Comp Stat Data Anal 53:3358-3371.

Hay SI, Snow RW, Rogers DJ, 1998. Predicting malaria seasons in Kenya using multitemporal meteorological satellite sensor data. Trans R Soc Trop Med Hyg 92:12-20.

Held L, Schrödle B, Rue H, 2010. Posterior and cross-validatory predictive checks: a comparison of MCMC and INLA. In:

Kneib T, Tutz G (eds) Statistical Modelling and Regression Structures. Physica-Verlag, 91-110 pp.

Huete A, Didan K, Miura T, Rodriguez EP, Gao X, Ferreira LG, 2002. Overview of the radiometric and biophysical performance of the MODIS vegetation indices. Remote Sens Environ 83:195-213.

IRI/LDEO Climate data library, 2016a. Climate Prediction Center - gridded precipitation estimates. Available from: https://iridl.ldeo.columbia.edu/SOURCES/.NOAA/.NCEP/.CPC/?Set-Language=en

IRI/LDEO Climate data library, 2016b. USGS – Africa Data Dissemination Service.Available from:https://iridl.ldeo.columbia.edu/SOURCES/.USGS/?Set-Language=en

IRI/LDEO Climate data library, 2017. NGDC – Gridded 1-km, quality controlled global Digital Elevation Model (DEM) data from the Global Land One-km Base Elevation (GLOBE) project. Available from:https://iridl.ldeo.columbia.edu/SOURCES/.NOAA/.NGDC/?Set-Language=en

Johnson JM, Clarke KC, 2021. An area preserving method for improved categorical raster resampling. Cartogr Geogr Inf Sci 48:292-304.

Kasasa S, Asoala V, Gosoniu L, Anto F, Adjuik M, Tindana C, Smith T, Owusu-Agyei S, Vounatsou P, 2013. Spatio-temporal malaria transmission patterns in Navrongo demographic surveillance site, northern Ghana. Malar J 12:63.

Kiani B, Thierry B, Apparicio P, Firth C, Fuller D, Winters M, Kestens Y, 2024. Associations between gentrification, census tract-level socioeconomic status, and cycling infrastructure expansions in Montreal, Canada. SSM Popul Health 25:101637.

Li T, Yang Z, Wang M, 2013. Temperature, relative humidity and sunshine may be the effective predictors for occurrence of malaria in Guangzhou, southern China, 2006–2012. Parasit Vectors 6:155.

Maharaj R, Seocharan I, Qwabe B, Mkhabela M, Kissoon S, Lakan V, 2019. Decadal epidemiology of malaria in KwaZulu-Natal, a province in South Africa targeting elimination. Malar J 18:368.

Matsushita B, Yang W, Chen J, Onda Y, Qiu G, 2007. Sensitivity of the Enhanced Vegetation Index (EVI) and Normalized Difference Vegetation Index (NDVI) to topographic effects: A case study in high-density cypress forest. Sensors 7:2636-51.

Midekisa A, Beyene B, Mihretie A, Bayabil E, Wimberly MC, 2015. Seasonal associations of climatic drivers and malaria in the highlands of Ethiopia. Parasit Vectors 8:1-11.

Midekisa A, Senay G, Henebry GM, Semuniguse P, Wimberly MC, 2012. Remote sensing-based time series models for malaria early warning in the highlands of Ethiopia. Malar J 11:165.

Moonasar D, Maharaj R, Kunene S, Candrinho B, Saute F, Ntshalintshali N, Morris N, 2016. Towards malaria elimination in the MOSASWA (Mozambique, South Africa and Swaziland) region. Malar J 15:419.

Moonasar D, Nuthulaganti T, Kruger PS, Mabuza A, Rasiswi ES, Benson FG, Maharaj R, 2012. Malaria control in South Africa 2000–2010: beyond MDG6. Malar J 11:294.

Mordecai EA, Caldwell JM, Grossman MK, Lippi CA, Johnson LR, Neira M, Rohr JR, Ryan SJ, Savage V, Shocket MS, Sippy R, Stewart AM, Thomas MB, Villena O, 2019. Thermal biology of mosquito-borne disease. Ecol Lett 22:1690-1708

Morris N, Frean J, Baker L, Ukpe IS, Barnes KI, Kruger P, 2013. Re-defining the extent of malaria transmission in South Africa: implications for chemoprophylaxis. S Afr Med J 103:861-4.

Musenge E, Chirwa TF, Kahn K, Vounatsou P, 2013. Bayesian analysis of zero inflated spatiotemporal HIV/TB child mortality data through the INLA and SPDE approaches: applied to data observed between 1992 and 2010 in rural North East South Africa. Int J Appl Earth Obs Geoinf 22:86-98.

Musal M, Aktekin T, Bayesian spatial modeling of HIV mortality via zero-inflated Poisson models. Stat Med 32:267-281.

Neelon BH, O'Malley AJ, Normand SLT, 2010. A Bayesian model for repeated measures zero-inflated count data with application to outpatient psychiatric service use. Stat Model 10:421-39.

Ntzoufras I, 2008. Bayesian Modeling Using WinBUGS, John Wiley & Sons, 520 pp.

Nygren D, Stoyanov C, Lewold C, Mansson F, Miller J, Kamanga A, Shiff CJ, 2014. Remotely-sensed, nocturnal, dew point correlates with malaria transmission in Southern Province, Zambia: a time-series study. Malar J 13:231.

Raman J, Gast L, Balawanth R, Tessema S, Brooke B, Maharaj R, Munhenga G, Tshikae P, Lakan V, et al., 2020. High levels of imported asymptomatic malaria but limited local transmission in KwaZulu-Natal, a South African malaria-endemic province nearing malaria elimination. Malar J 19:152.

Rue H, Martino S, Chopin N, 2009. Approximate Bayesian inference for latent Gaussian models by using integrated nested Laplace approximations. J R Stat Soc B 71:319-92.

Sikaala CH, Dlamini B, Lungu A, Fakudze P, et al., 2024. Malaria elimination and the need for intensive inter-country cooperation. A critical evaluation of regional technical co-operation in Southern Africa. Malar J 23:62.

Sinka ME, Pironon S, Massey NC, Willis KJ, 2020. A new malaria vector in Africa: Predicting the expansion range of Anopheles stephensi and identifying the urban populations at risk. PNAS 117:24900-24908.

Sogoba N, Vounatsou P, Bagayoko MM, Doumbia S, Dolo G, Gosoniu L, Traore SF, Toure YT, Smith T, 2007. The spatial distribution of Anopheles gambiae sensu stricto and An. arabiensis (Diptera: Culicidae) in Mali. Geospat Health 1:213-22.

South Africa National Department of Health, 2012. Malaria elimination strategy for South Africa 2012-2018. Pretoria, South Africa National Department of Health.

Spiegelhalter DJ, Best NG, Carlin BP, Van Der Linde A, 2002. Bayesian measures of model complexity and fit. J R Stat Soc B 64: 583-639.

Stefani A, Dusfour I, Corrêa APS, Cruz MC, Dessay N, Galardo AK, Galardo CD, Girod R, Gomes MS, Gurgel H, Lima ACF, Moreno ES, Musset L, Nacher M, Soares AC, CarmeB, Roux E, 2013. Land cover, land use and malaria in the Amazon: a systematic literature review of studies using remotely sensed data. Malar J 12:192.

Tatem AJ, Gething PW, Smith DL, Hay SI, 2013. Urbanisation and the global malaria recession. Malar J 12:133.

Tatem AJ, Guerra CA, Kabaria CW, Noor AM, Hay SI, 2008. Human population, urban settlement patterns and their impact on Plasmodium falciparum malaria endemicity. Malar J 7:218.

Tsoka-Gwegweni JM, 2022. Status of malaria and its implications for elimination in an endemic province of South Africa: retrospective analysis. Pan Afr Med J 41:275.

Tusting LS, Willey B, Lucas H, Thompson J, Kafy HT, Smith R, Lindsay SW, 2013. Socioeconomic development as an inter-

vention against malaria: a systematic review and meta-analysis. Lancet 382:963-72.

Villena OC, Arab A, Lippi CA, Ryan SJ, Johnson LR, 2024b. Influence of environmental, geographic, socio-demographic, and epidemiological factors on presence of malaria at the community level in two continents. Sci Rep 14:16734.

Villena OC, McClure KM, Camp RJ, LaPointe DA, Atkinson CT, Sofaer HR, Fortini LB 2024a. Environmental and geographical factors influence the occurrence and abundance of the southern house mosquito, Culex quinquefasciatus, in Hawai'i. Sci Rep 14:604.

Villena OC, Ryan SJ, Murdock CC, Johnson LR, 2022. Temperature impacts the environmental suitability for malaria transmission by Anopheles gambiae and Anopheles stephensi. Ecology 103:e3685.

Viña A, Henebry GM, Gitelson AA, 2004. Satellite monitoring of vegetation dynamics: Sensitivity enhancement by the wide dynamic range vegetation index. Geophys Res Lett 31:L04503.

White MT, Griffin JT, Churcher TS, Ferguson NM, Basáñez MG, Ghani AC, 2011. Modelling the impact of vector control interventions on Anopheles gambiae population dynamics. Parasit Vectors 4:153.

World Health Organization, 2023. World malaria report 2023. Geneva, Switzerland. Available from: https://www.who.int/teams/global-malaria-programme/reports/world-malaria-report-2023

World Health Organization, 2024. World malaria report 2024: addressing inequity in the global malaria response. Geneva, Switzerland. Available from: https://www.who.int/teams/global-malaria-programme/reports/world-malaria-report-2024

Yé Y, Louis VR, Simboro S, Sauerborn R, 2007. Effect of meteorological factors on clinical malaria risk among children: an assessment using village-based meteorological stations and community-based parasitological survey. BMC Public Health 7:101.

Zayeri F, Salehi M, Pirhosseini H, 2011. Geographical mapping and Bayesian spatial modeling of malaria incidence in Sistan and Baluchistan province, Iran. Asian Pac J Trop Med 4:985-992.

Zianni MR, Nikbakhtzadeh MR, Jackson BT, Panescu J, Foster WA, 2013. Rapid discrimination between Anopheles gambiae s.s. and Anopheles arabiensis by high-resolution melt (HRM) analysis. J Biomol Tech 24:1-7.

Zinszer K, Kigozi R, Charland K, Dorsey G, Brewer TF, Brownstein JS, Kamya MR, Buckeridge DL, 2015. Forecasting malaria in a highly endemic country using environmental and clinical predictors. Malar J 14:245.

Zinszer K, Talisuna AO, 2022. Fighting insecticide resistance in malaria control. Lancet Infect Dis 23:138-9.